 DOI: 10.1002/masy.201450307

Design and Viscoelastic Properties of PDMA/Silica Assemblies in Aqueous Media

*Laurence Petit, Linn Carlsson, Séverine Rose, Alba Marcellan, Tetsuharu Narita, Dominique Hourdet**

Summary: Based on specific interactions taking place between poly(*N,N*-dimethylacrylamide) [PDMA] and silica nanoparticles, two strategies were used to improve the viscoelastic properties of aqueous formulations. First, PDMA oligomers were grafted onto a non-adsorbing poly(acrylamide-co-sodium acrylate) backbone. With this architecture, the binding process of PDMA side-chains with silica nanoparticles was shown to proceed very similarly to free PDMA chains and to promote the formation of hybrid physical networks. The viscoelastic properties of these systems are controlled by the concentration of inorganic cross-links and the fraction of adsorbing grafts involved in the formation of bridges between particles. An optimum weight ratio between silica and grafts was found for the viscoelastic properties, in agreement with the saturation of silica beads by the PDMA precursor. While the homogeneous formation of such hybrid assemblies remains limited to mixtures involving low polymer concentrations ($\leq$ 2 wt%), we show that homogeneous hybrid networks can be readily prepared by direct polymerization of DMA monomer ($\geq$ 5 wt%), with or without chemical cross-linker, in a suspension of silica nanoparticles. In this case, the specific interactions taking place between the silica filler and the whole polymer network give rise to a very unusual combination of properties where elasticity, dissipation, strength and strain at failure are enhanced simultaneously. While the intrinsic structure of the network can be controlled by the level of chemical cross-linking, physical interactions dominate the dissipation process with a dramatic time dependence of the mechanical properties.

Keywords: hybrid network; hydrogel; poly(dimethylacrylamide); self-assemblies; silica

Introduction

Aqueous-based polymer formulations with high viscoelastic and self-healing properties at moderate concentrations find important applications in a wide range of domains like cosmetics, paints and drilling fluids.[1–3] In most cases, enhanced properties are obtained through the formation of transient networks in complex systems involving macromolecular self-assemblies. In water, hydrophobic interactions play a major role and alkyl, perfluoroalkyl, aromatic or polyacrylate stickers have been widely used to develop water-soluble associating polymers.[4–17] The synthesis of hydrophobically modified graft or telechelic architectures, together with their self-assembling properties in semi-dilute aqueous solutions, have been extensively studied on both theoretical and experimental points of view and some of these polymers have known successful developments like Hydrophobic Ethoxylated URethane (HEUR) and Hydrophobically modified Alkali Swellable Emulsions (HASE). In aqueous media, the spectrum of interactions is very broad and electrostatic complexation or hydrogen bonding can also be considered as driving forces for self-association. Such assemblies can involve macromolecular species (like polymer complexes), polymer and small molecules or ions (like poly(vinyl alcohol)/

Laboratoire Sciences et Ingénierie de la Matière Molle (SIMM), UMR 7615 CNRS/UPMC/ESPCI ParisTech, 10 rue Vauquelin, F-75231 Paris Cedex 05, France
E-mail: dominique.hourdet@espci.fr

borax or calcium alginates), or polymer and colloids.[18–21] For instance, taking advantage of the adsorption of some polymers with silica surfaces in aqueous environment, we have shown that homogeneous physical networks could be obtained by simply mixing silica nanoparticles with a non-interacting polymer grafted with adsorbing grafts.[22–24] A schematic picture of such hybrid assembly is given in Figure 1 in the case of poly(*N,N*-dimethylacrylamide) [PDMA].

While self-assembly has been widely studied in liquid formulations during at least the last 3 decades, it is only during the last 10 years that this knowledge has been transposed to covalent hydrogels. Indeed, while these soft materials are used in many bio-applications[25–28] such as superabsorbants, contact lenses, bio-sensors for encapsulation and drug delivery systems, scaffolds for tissue engineering, they are intrinsically brittle and the reinforcement of their mechanical behavior remains a critical issue. For that purpose, several strategies have been considered using improved architectures like double networks,[29] slide-ring gels,[30] topological gels[31] but a very versatile method consists in introducing dissipation process in the covalent network playing with the same physical interactions as reported with associating polymers. This is the case for instance with hydrophobically modified hydrogels which show a steep increase of dissipation processes, due to the deformation of hydrophobic associations under stress, with a large increase of their limit extensibility and resistance to crack propagation.[32–34] There are other examples of successful development of tough hydrogels, coupling covalent bonds and weak interactions, but one cannot miss the work of Haraguchi and co-workers[35,36] who developed highly extensible nano-composite gels (NC gels) by polymerizing *N*-alkylacrylamide monomers in the presence of exfoliated clay platelets. These NC gels showed very high stiffness and deformability (until 1000%) that can be tuned with their formulation.

In a similar way, we have modified our initial strategy based on the formulation of hybrid assemblies by polymerizing the adsorbing monomer (DMA) directly in the silica suspension[37] (see Figure 1). A small amount of chemical cross-linker can be added in order to fix the 3D topology and the mechanical properties of the material, tuning the system from a viscoelastic liquid to a viscoelastic solid.[38,39]

In the present paper, we aim at reviewing and comparing the two strategies that we developed to design hybrid assemblies based on PDMA/silica interactions. Using the same silica nanoparticles, we will show that the mixing procedure that involves putting together the graft copolymer and the particles is an efficient strategy as long as we work at low polymer concentration. The viscoelastic properties of hybrid formulations dramatically increase with the amount of inorganic crosslinkers and optimal properties are reached around the plateau value of the adsorption isotherm.

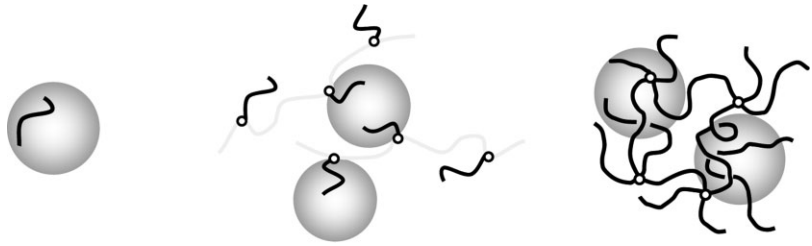

Figure 1.
From left to right, schematic representation in aqueous media of 1) PDMA chain adsorbed on a silica nanoparticle, 2) formation of hybrid assemblies between silica particles and PDMA side-chains grafted onto a non-adsorbing copolymer backbone, and 3) hybrid hydrogel with silica beads embedded into a covalently cross-linked PDMA network.

By comparison, the formation of hybrid hydrogels by copolymerizing DMA within the particle suspension is more suitable to prepare homogeneous formulations in a wide range of composition. In this case, we will show that the elastic properties, together with the dissipation process, can be tuned independently playing with the amount of chemical cross-linker and silica particles, respectively.

Experimental Part

Materials

N,N-dimethylacrylamide (DMA, 99%, Aldrich), potassium persulfate (KPS, Acros Organics), *N,N,N′,N′*-tetramethylethylenediamine (TEMED, 99.5%, Sigma Aldrich) and N,*N′*-methylenebisacrylamide (MBA, Fluka) were used as received without further purification. The graft copolymer poly(acrylamide-co-sodium acrylate)-g-poly(N,N-dimethylacrylamide) [PAMH-g-PDMA] has been obtained by coupling amino-PDMA telomer with carboxylic groups of the PAMH backbone as already reported in a previous paper.[24] The copolymer backbone, containing 70 mol% of acrylamide and 30 mol% of sodium acrylate, is characterised by a number average degree of polymerization $DP_n = 840$ ($Đ = 2.4$). The weight percentage of PDMA grafts ($DP_n = 113$ and $Đ \cong 2$) in the whole copolymer is 70 wt%, corresponding to an average number of 14 grafts per copolymer chain (1.6 graft/100 monomer units).

Two different batches of silica nanoparticles (Ludox TM50 from Dupont) were used in this work. In the case of hybrid formulations prepared by mixing graft copolymers and inorganic material, the silica suspension was purified by continuous ultrafiltration with water at pH = 8 (membrane cut-off = 10 kD). Fresh and stable suspensions of negatively charged particles were obtained at concentrations between 25 and 160 g/L (pH = 8). The characterization of silica particles by small angle neutron scattering (SANS), gave a mean radius $R_0 = 150$ Å with low polydispersity. The corresponding specific area was taken as $S_{spe} = (3/\rho_{Si}R) = 87\ m^2.g^{-1}$ considering a specific weight $\rho_{Si} = 2.3\ g.mL^{-1}$. In the case of hybrid hydrogels, prepared by radical polymerization of DMA in the presence of silica suspension, the latter was used as received (52 wt% and pH = 9) without further purification in order to reach higher amounts of particles in the final formulation. The characterization of this silica suspension by SANS and SEM gives, respectively, a mean radius $R_0 = 135$-140 Å.

Preparation of Hybrid Assemblies

Hybrid formulations were prepared by mixing silica suspension with the copolymer solution initially equilibrated at pH = 8. Due to the strong interactions taking place between copolymer chains and silica particles, the mixtures were kept under gentle stirring for 10 days and then at rest during 3 additional days before experiments. In these conditions, the viscoelastic properties were reproducible for all the mixtures studied up to $C_p = 20\ g{\cdot}L^{-1}$; C_{si} varying between 0 and $90\ g{\cdot}L^{-1}$.

Preparation of Hydrogels

Hydrogels were prepared in a glove box at 25 °C by free-radical polymerization (under nitrogen atmosphere) of DMA and MBA in an aqueous suspension of silica nanoparticles using KPS and TEMED as redox initiators.[37] The gelation process takes place into home-made moulds consisting of two covered glass plates ($L_0 = 690$ mm, $w_0 = 40$ mm) spaced by a stainless steel spacer of 2 mm thick (t_0). After 24 hours, hydrogels were removed from the mould and immediately characterized, or stored into paraffine oil to prevent samples from drying before analysis. For all the syntheses, the molar ratio (DMA)/(KPS)/(TEMED) was set equal to 100/1/1 while the relative amounts of DMA, MBA, silica and water were varied keeping constant the weight ratio Polymer/Water (PW). The nomenclature of hydrogels is SPx_PWy_Rz; with S for Silica, P for Polymer, W for Water and R for the level of crosslinking. x is the weight ratio between silica and polymer (varying between 0 and 5), y is the weight

ratio between polymer and water (equal to 0.14) and z is the MBA/DMA molar percentage with z = 0, 0.1 and 1 mol%.

Adsorption Measurements

Different series of polymer/silica mixtures (pH = 8) were prepared in centrifuge vials by introducing increasing amounts of PDMA into a silica suspension of fixed concentration ($C_{Si} = 5\ g{\cdot}L^{-1}$). The samples were stored under gentle stirring during 72 hours and the silica material was settled down by centrifugation at 25000 g during 12 hours at T = 20 °C. The supernatant was recovered and submitted once again to the same centrifugation procedure. The total concentration of free polymer chains in the supernatant (C_P^e) was determined by titration of the Total Organic Carbon using a TOC Carbon Analyser DC-80 (Tekmar Dohrmann). The same experimental procedure was used for each polymer concentration and two measurements were made each time.

Swelling Measurements

For each sample, small pieces of hydrogel in the preparation state were initially cut, weighted and then placed at room temperature into a glass container with a large excess of solvent (lithium nitrate 0.5 $mol{\cdot}L^{-1}$). The solution was changed every day during 10 days and the gels swollen at equilibrium were finally weighted. The equilibrium swelling ratio (Q_e) of the hydrogels in salted environment were calculated as the volume ratio between the hydrated polymer (polymer + solvent) and the dried polymer; the silica being not considered in the calculation.

Rheology

Viscoelastic properties of aqueous copolymer solutions, without or with added silica particles (0–90 $g{\cdot}L^{-1}$), were carried out at 20 °C on a controlled stress rheometer (Haake RS150) using a cone/plate geometry. In order to explore a wide range of viscoelastic properties, the experimental conditions were fixed, after a first investigation within the linear domain, at $\sigma = 1$–5 Pa and constant frequency ($freq = 1$ Hz). In these conditions, storage (G') and loss (G'') moduli as well as complex viscosity ($\eta*$) were determined. Complementary experiments were also performed by scanning the frequency in the linear domain.

Mechanical Testing

Tensile tests were performed with hybrid hydrogels on a standard tensile Instron machine, model 5565. The device used a 10 N load cell and a video extensometer which follows the local displacement up to 120 mm. The sample dimensions were $L_0 = 25$–30 mm, $w_0 = 5$ mm and $t_0 = 2$ mm. Gel samples were placed in home-made screw side action grips and marked by two white dots for monitoring with the video extensometer. Strain was obtained from the optical extensometer and defined as the ratio $(l\text{-}l_0)/l_0$, where l and l_0 are respectively the length during stretching and the initial distance between dots. The nominal stress was calculated from the tensile force divided by the initial cross section area (5×2 mm^2). Monotonic tensile tests and loading-unloading cycles were carried out at room temperature at a nominal strain rate $\dot{\varepsilon} = 0.06\ s^{-1}$ (around 100 mm/min) in order to characterize the modulus and the dissipated strain energy (hysteresis). Loading-unloading cycles were applied from 0 to a maximal nominal strain ($\varepsilon_0 = 0.1$) at a constant strain rate.

Small Angle Neutron Scattering (SANS)

SANS experiments were performed at Laboratoire Léon Brillouin (CEA-Saclay, France) with spectrometer PACE dedicated to isotropic analyses. Contrast matching experiments were carried out with hybrid hydrogels initially prepared with a H_2O/D_2O volume ratio of 0.78/0.21 that matches the contribution of the organic matrix: $\rho_s = \rho_{PDMA} = 0.94\ 10^{-6}$ $Å^{-2}$; ρ_s and ρ_{PDMA} being the scattering length densities of the solvent and PDMA, respectively. From hydrogel plates in their preparation state, discs (diameter $d = 14$ mm and thickness $t = 1$ or 2 mm) were cut with a cylindrical punch and placed between two quartz slides

hermetically sealed for SANS analyses. Absolute scattering intensities ($I(q)$ in cm^{-1} or 10^{-8} $Å^{-1}$), obtained from the standard procedures, were normalized as follows:

$$I_{cor}(q) = \frac{2\pi^2}{Q_{\exp}} I(q) = P(q).S(q) \quad (1)$$

with $Q_{\exp} = \int_0^\infty q^2 I(q) dq$ the experimental invariant, $P(q)$ the form factor of the particles and $S(q)$ their structure factor.

Two experimental configurations were used, keeping constant the sample-to-detector distance $D = 4.7$ m and changing the wavelength of the incident neutron beam from $\lambda = 12$ to 4.5 Å. The corresponding values of the scattering vector modulus are ranging between 0.0034 and 0.098 $Å^{-1}$.

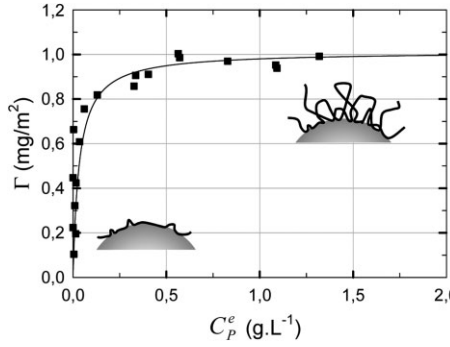

Figure 2.
Adsorption isotherm of PDMA (■) on silica particles at T = 20 °C. The solid line is the theoretical fit obtained from the Langmuir isotherm: $\Gamma^{-1} = \Gamma_{\max}^{-1}(1 + K^{-1}C_P^{-1})$, with $\Gamma_{max} = 1$ mg·m^{-2} the maximum amount adsorbed and $K = 30$ L·g^{-1} the Langmuir equilibrium constant.

Results and Discussion

Hybrid Assemblies

Adsorption Behaviour of PDMA Chains with Silica Surfaces

As previously mentioned, the adsorption experiments of PDMA on silica beads were carried out during 3 days in order to let enough time for adsorption and reorganisation of chains on the particles. The amount of adsorbed polymer on silica surfaces (Γ in mg·m^{-2}) is plotted against the equilibrium polymer concentration C_P^e in Figure 2.

The isotherm clearly evidences that PDMA chains readily interact with silica, with a strong adsorption regime at low coverage of the particles; the adsorbed amount of polymer increasing sharply for $\Gamma < 0.7$ mg·m^{-2}. As previously reported,[24] this first regime corresponds to the adsorption of PDMA chains in a flat conformation (high proportion of trains compared to loops and tails) with a maximum of monomer units interacting directly with the surface. This regime is followed by a weaker interaction domain ($\Gamma > 0.7$ mg·m^{-2}) where the adsorption of polymer chains involves a decreasing fraction of trains with the formation of larger loops and tails. This regime finally reaches a plateau value at $\Gamma_{max} \cong 1$ mg·m^{-2} that roughly corresponds to the saturation of particles with a weight ratio between silica and PDMA: $(SP)_0 \cong 11$-12. The high adsorption constant ($K = 30$ L·g^{-1}), obtained from the Langmuir isotherm model applied in the high coverage regime (Figure 2), can be correlated to the strong binding energy of PDMA with silica surfaces. It can be noticed that contrary to polyacrylamide that has almost no affinity for silica[40] (the adsorbed amount being very low), the strong adsorption of PDMA originates from the coupling between carbonyl/silanol hydrogen bonding and hydrophobic interactions between methyl groups and silica surface.[41,42] From a general point of view, this behaviour that is classically observed with poly(N-alkylacrylamide) derivatives is widely used in the field of capillary electrophoresis to suppress the electroosmotic flow in fused silica capillaries.

Hybrid Assemblies between PAMH-g-PDMA and Silica Nanoparticles

The viscoelastic properties of ternary hybrid mixtures "PAMH-g-PDMA/silica/H_2O" were studied at $T = 20$ °C for a large range of silica and copolymer concentrations. Starting initially with binary

systems of very low viscosity, either copolymer solutions or silica suspensions, a huge increase of viscoelasticity is observed when organic and inorganic materials are mixed together. By comparison, the addition of silica particles into a solution of the polymer backbone (PAMH) does not show any significant modification of the rheological behaviour. From SANS experiments, it was shown that the structure factor of silica particles remains practically unchanged in the presence of copolymer, indicating that the particles remain stable and well dispersed even when hybrid assemblies are formed. For a set of formulations, prepared at a fixed copolymer concentration ($C_p = 20\,\text{g.L}^{-1}$), the viscoelastic behaviour shown in Figure 3 clearly highlights the formation of a percolating network with silica particles interconnecting graft copolymer chains.

At low concentration of added silica particles ($C_{Si} < 20\,\text{g.L}^{-1}$), the number of inorganic junctions between polymer chains remains too low to reach the percolation threshold and the solution behaves mainly as a viscous liquid with isolated clusters. In the range $C_{Si} = 18\text{-}20\,\text{g·L}^{-1}$, where G' and G'' cross each other, the hybrid formulation reaches the gel point (C_{Si}^{Gel}).

This conclusion is also supported by the fact that in these conditions G' and G'' also follow the same frequency dependence.[24,43] At higher silica concentrations, the hybrid mixtures mainly behave as chemical gels with very weak frequency dependence of dynamic moduli and no relaxation process in the range of observation ($t = 10^{-2}$ to 10 s). This result is consistent with the high binding energy between PDMA side-chains and silica surfaces; the life time of physical associations being out of scale in our experiments. In these conditions, hybrid assemblies can be considered as frozen, as in the case of covalent networks, and the elastic modulus (G') can be used to determine the concentration of elastically active chains (ν) from $G' \cong RT\nu$ assuming that the contribution of chain entanglements remains negligible at this polymer concentration. Then taking into account the number of silica particles (n) in

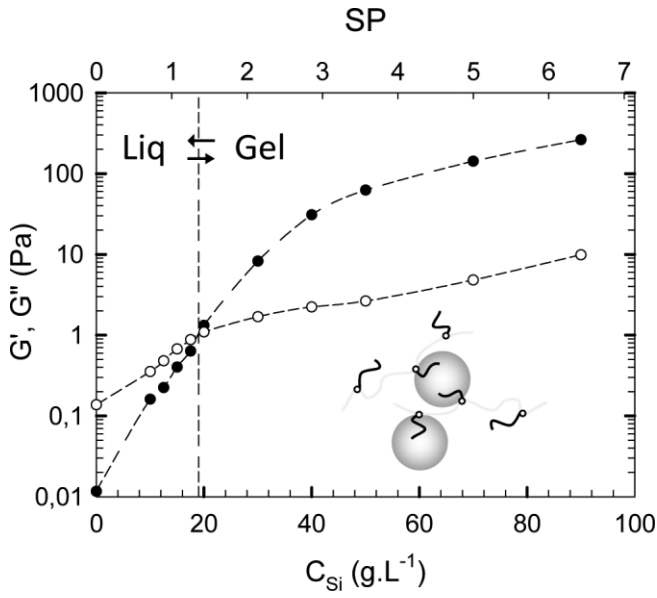

Figure 3.
Influence of silica concentration on viscoelastic properties {G' (●) and G'' (○)} of PAMH-g-PDMA aqueous solutions ($C_p = 20\,\text{g·L}^{-1}$, $freq = 1$ Hz and $T = 20\,^{\circ}\text{C}$). The weight ratio between silica and PDMA (SP) is also given on top x-axis.

the mixture, the average elastic functionality of particles ($f = 2\nu/n$) can be calculated considering that the formation of one elastic bridge involves two particles (Table 1). In these conditions, where all the formulations were prepared with an excess of PDMA side-chains with respect to silica (SP < 12), the average functionality of particles always increases with silica concentration.

As shown in previous papers,[22,24] the formation of hybrid assemblies follows fairly well the percolation theory and their formation can be seen as the percolation of macromolecular chains through inorganic cross-linkers or, conversely, as the percolation of inorganic clusters through macromolecular connectors. Taking into account the concentration of inorganic cross-linkers as the main variable, we can see in Table 2, that the silica concentration threshold (C_{Si}^{gel}) decreases with decreasing copolymer concentration. Nevertheless, if we consider that the formation of an elastic chain requires that two PDMA side-chains, belonging to the same backbone, have to bridge two different particles, there is obviously a critical silica concentration below which the system cannot percolate: the extended polyelectrolyte chain being too small to connect the particles. From a simple calculation based on the dimension of the copolymer chain, this critical silica concentration is expected at $\left(C_{Si}^{Gel}\right)_{\min} \cong 6\,\mathrm{g{\cdot}L^{-1}}$.[24]

Using the whole series of viscoelastic data, obtained from various concentrations of copolymer and silica nanoparticles, the variation of the elastic modulus versus the copolymer concentration has been plotted in Figure 4a. Interestingly, one can notice that 1) for a fixed silica concentration the elastic modulus reaches a maximum at a given copolymer concentration and 2) this maximum is shifted towards lower copolymer concentration for lower silica content. At first, these results could appear quite confusing as working at a fixed silica concentration, let's take $15\,\mathrm{g.L^{-1}}$ for instance, the elastic modulus decreases 50 times when the polymer concentration increases 10 times! Nevertheless, taking into account the driving force of the self-assembling process, i.e. the adsorption of PDMA chains on silica particles, it appears that the weight ratio SP between these two components (the level of particle coverage), is really the key parameter to consider. As a matter of fact, when the elastic modulus is plotted versus the weight ratio SP (Figure 4b), all the maxima of the curves gather around the same value (SP≅10) that roughly corresponds to the saturation of silica surfaces with PDMA chains.

Below this "stoichiometric ratio", there are less silica beads able to bridge copolymer chains through PDMA stickers and the viscoelastic properties progressively fall down. In the middle range (SP ≅ $(SP)_0$), close to the saturation of silica surfaces by PDMA stickers, all the conditions are put together to get the maximum number of connections between silica surfaces and PDMA stickers. On the other hand, with an excess of silica particles (SP > $(SP)_0$) there will be less polymer chains available to percolate the inorganic beads and the hydrogel will progressively become weaker, eventually with the formation of isolated aggregates. This feature is somewhere similar to the case of hydrophobically modified polymer solutions prepared with

Table 1.
Elastic modulus (G') and average elastic functionality of particles (f) as a function of silica concentration ($C_p = 20\,\mathrm{g{\cdot}L^{-1}}$).

C_{Si} ($\mathrm{g{\cdot}L^{-1}}$)	SP	G' (Pa)	f
30	2.1	9	5
40	2.9	36	14
50	3.6	68	22
70	5	152	34
90	6.4	291	52

Table 2.
Silica concentration threshold (C_{Si}^{gel}) for the sol/gel transition in ternary hybrid mixtures: PAMH-g-PDMA/silica/H_2O.

C_p ($\mathrm{g{\cdot}L^{-1}}$)	C_{Si}^{Gel} ($\mathrm{g{\cdot}L^{-1}}$)
20	18
10	12.5
7.5	10
5	8

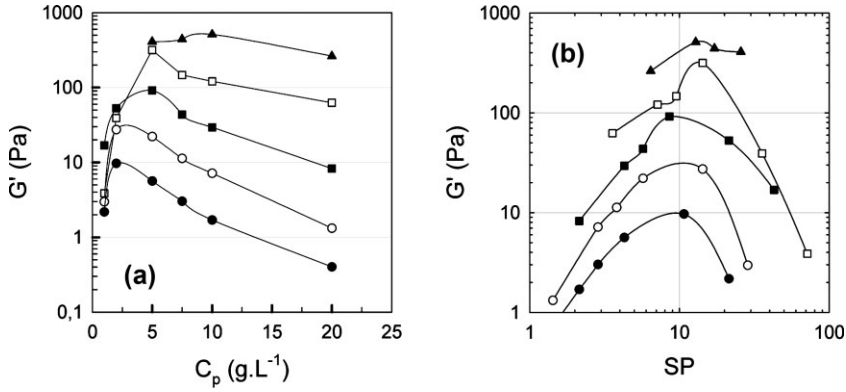

Figure 4.
Variation of the elastic modulus (G') versus a) the copolymer concentration (C_p) and b) the weight ratio silica/PDMA (SP) for various series of silica concentrations: 15 (●), 20 (○), 30 (■), 50 (□) and 90 g·L^{-1} (▲).

added surfactant,[44] where the role of silica beads is played by the surfactant micelles which are able to bind hydrophobic stickers from different copolymer chains.

The formation of hybrid assemblies can be discussed further by using the schematic picture given in Figure 5. For $SP \geq (SP)_0$, one can assume that part of PDMA side-chains self-associate with silica surfaces forming loops and bridges, while others still behave as pendant chains. The proportion of these pendant chains increases with increasing amount of copolymer above $(SP)_0$. From the point of view of viscoelasticic properties, only inter-particle bridges formed between two adsorbed side-chains belonging to the same backbone will contribute to the elasticity of the network (elastically active chains).

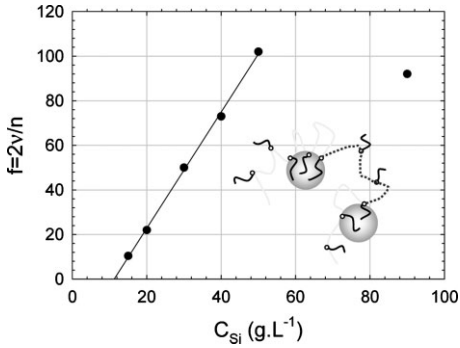

Figure 5.
Variation of the average elastic functionality of particles (f) versus the concentration of particles for hybrid formulations corresponding to $SP \cong (SP)_0$ or $C_{Si} = (SP)_0.C_{PDMA}$. The dotted part of the copolymer chain illustrates the formation of an elastic bridge between two particles.

As we can see in Figure 5, the average elastic functionality of particles is proportional to the amount of added particles and polymer up to $C_{Si} = 50\,g{\cdot}L^{-1}$. In these conditions the increase of the "elastic functionality" of silica particles mainly comes from the transformation of loops into bridges with increasing silica and polymer concentrations; SP being fixed in that case to $(SP)_0$. Interestingly, one can extrapolate the absence of elastic properties for silica and polymer concentrations below 10 and 1 g·L^{-1}, respectively, in good agreement with the calculated value based on geometrical considerations ($(C_{Si}^{Gel})_{min} = 6\,g{\cdot}L^{-1}$). The discrepancy observed at $C_{Si} = 90\,g{\cdot}L^{-1}$ could be attributed to the increasing difficulty to form homogeneous networks in the equilibrium state at such high particle concentration. Moreover, if we consider that each particle is able to bind a maximum of 150 PDMA side-chains (based on $\Gamma_{max} = 1\,mg/m^2$), and that each PDMA sticker can participate to 0, 1 or 2 elastically active chains, we can see that the average elastic functionality of particles plotted in Figure 5 are quite high for $C_{Si} = 50\text{-}90\,g.L^{-1}$ ($f \cong 100$); the maximum

being expected around $f_{max} \approx 2 \times 150 \approx 300$. According to this simple picture, it is reasonable to assume that such a high ideal connectivity cannot be reached easily for steric and entropic reasons and that the so-called average functionality of particles should level off well below f_{max}.

Finally, the self-assembling behaviour of hybrid formulations is summarized in Figure 6 where the elastic modulus has been replaced by the dynamic viscosity in order to cover all the formulations, elastic or not. Here, the complex viscosity of the ternary mixtures, normalised by the viscosity of the copolymer solution without added silica (η^*/η_0^*), has been plotted in a 2D mapping against copolymer and silica concentrations. This representation clearly shows the relative influence of organic and inorganic materials on the self-assembling behaviour of the ternary mixtures.

By adding a small amount of particles into the copolymer solutions, the mixtures rapidly turn from a liquid to a viscoelastic gel and we can see on the left side of the diagram that the sol/gel transition line fits approximately with a 10-times increase of the complex viscosity. The same holds when a small amount of copolymer is added into the silica suspension and the mixtures rapidly become viscoelastic above $C_p = 1\,\mathrm{g{\cdot}L^{-1}}$. Moreover, if one compares the rise of viscosity obtained by mixing the graft copolymer with the silica nanoparticles, there is a range of optimal formulations that corresponds approximately to the "stoichiometry" of the complex silica/PDMA as determined from the adsorption isotherm: $(SP)_0 \cong 12$ (white line in Figure 6). From this ternary diagram, one can extrapolate that hybrid assemblies with very strong viscoelastic properties could be obtained at higher polymer concentrations following the same arguments but the main problem comes from the difficulty to prepare homogeneous mixtures.

As previously mentioned, all our experiments were limited to $C_p = 20\,\mathrm{g{\cdot}L^{-1}}$ in order to prepare homogeneous and reproducible samples within two weeks; going further is not conceivable using the same procedure. In order to avoid this problem, it is reasonable to start from weakly interacting formulations that can be modified afterwards and two strategies can be considered: 1) polymerizing a silica precursor, like tetraethyl orthosilicate in a solution of PDMA chains or grafted copolymer or 2) polymerizing DMA monomer, with or without comonomer, in the presence of silica particles.

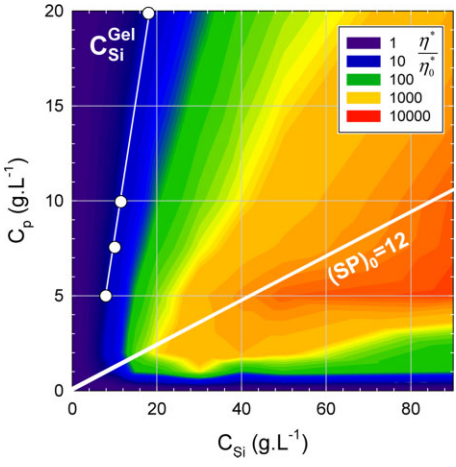

Figure 6.
Projection of the complex viscosity of the ternary mixtures, normalised by the viscosity of the copolymer solution without added silica (η^*/η_0^*), against copolymer and silica concentrations.[24] The white symbols give the limits of the sol/gel transition reported in Table 2 and the white thick line indicates the weight ratio of silica/PDMA obtained from the plateau value of the adsorption isotherm.

Hybrid Hydrogels

Preparation

In order to keep working in aqueous media with homogeneous formulations containing high amounts of organic and inorganic materials, the polymerization of the organic network in the silica suspension has been preferred. For that purpose the polymerization process of DMA in water has been studied in details[37] and it was shown that transfer reactions between the radical initiator and methyl groups of DMA were responsible for self-crosslinking reactions giving rise to branched structures and weak 3D hydrogels depending on the polymer

concentration. In order to get homogeneous gels, we systematically worked well above the critical gelation threshold ($C_{Pl}^{Gel} \cong 50\,g{\cdot}L^{-1}$) and the weight ratio polymer/water (PW) was fixed at $y = 0.14$ which corresponds to a polymer concentration $C_p = 125\,g{\cdot}L^{-1}$ or a swelling ratio in the preparation state $Q_0 = 8.5$. In order to investigate the impact of the elastic network on the mechanical properties of hybrid hydrogels, different amounts of chemical cross-linker (Rz) were used for the copolymerization: R0, R0.1 and R1, z being the molar percentage between MBA and DMA.

Structure

SANS experiments were carried out with contrast matching of PDMA matrix in order to investigate the structure of hybrid hydrogels and more particularly of the silica particles**.** As shown in Figure 7, where the scattering behaviour of hybrid networks SP2 and silica suspension are compared at the same filler concentration ($\phi = 0.1$), we get a very good superposition of the curves in the high q-range which is mainly dominated by the form factor of silica particles ($S(q) \cong 1$).

Conversely, the structure factor prevails in the low q-range where the scattering intensity increases with increasing level of cross-linking. By comparison with the silica suspension, the polymerization of DMA without cross-linker ($z = 0$ mol%) or with a low level of cross-linker ($z = 0.1$ mol%) only slightly increases the osmotic compressibility of the system which remains repulsive in nature. At higher level of cross-linking ($z = 1$ mol%), the potential between particles becomes less repulsive; the system becoming more compressible. During polymerization, the adsorption of PDMA chains at the surface of silica beads is responsible for the formation of an attractive potential between particles and we can reasonably expect that the heterogeneity of the hybrid network will increase with parameters such as binding energy or cross-linking density. Nevertheless, contrary to the aggregation behaviour reported by Shibayama and co-workers[45] during the polymerization of N-isopropylacrylamide at low pH (between 3 and 6) in the presence of silica particles, our hybrid hydrogels can be considered homogeneous for moderate level of cross-linking ($z = 0$-1 mol%). Moreover, from additional contrast matching experiments (not reported here), we did not observe any concentrated polymer layer at the silica surface. The conclusion is that, while PDMA chains formed by polymerization readily interact with silica particles as we will see afterwards, the relative concentration of the adsorbed layer remains in average close to the bulk concentration.

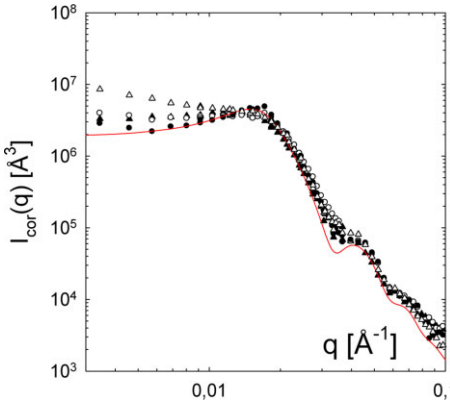

Figure 7.
Double logarithmic plot of the reduced scattering intensity of PDMA/silica hydrogels (SP2_PW0.14_Rz) prepared with different amounts of cross-linker: R0 (○), R0.1 (▲) and R1 (△). By comparison, the scattered intensity of silica particles without PDMA but at the same volume fraction ($\phi = 0.1$) and in the same solvent conditions is shown (●) with the fit (solid line) obtained from the model of polydisperse spheres interacting with hard sphere repulsions.[39]

Swelling Behaviour

It is important to notice that all the analyses performed during swelling experiments have shown 1) that the level of organic extractible (monomer and polymer studied by GPC) was negligible and 2) that after reaching the equilibrium, the organic/inorganic content (SPx) in the gel, determined by thermogravimetric analysis, was

unchanged; silica particles remain embedded inside the network after swelling.

The swelling ratio at equilibrium in ionic environment is plotted in Figure 8 for the three series of hybrid hydrogels (R0, R0.1 and R1).

In the absence of inorganic particles, we qualitatively observe the decrease of Q_e (120, 40 and 14) with the increasing level of cross-linking (R0, R0.1 and R1, respectively) as it is expected from the thermodynamic of hydrogels. More interestingly we can also notice that for each series, the swelling ratio at equilibrium decreases progressively with the amount of inorganic particles; the amplitude being more pronounced at low level of cross-linker. The swelling behaviour at equilibrium is a classical experiment in filled elastomers to investigate interactions between the organic network and the filler. In the case of attractive interactions between the polymer matrix and the filler, the swelling ability of the system will be reduced by geometrical constrains in comparison with the unfilled system. These situations have been analytically described by Berriot et al[46] using continuous media mechanics:

$$Q_e = \left[\left(Q_{ref}^{1/3} + \frac{3\left(1 - Q_{ref}^{1/3}\right)(1-\nu)}{2(1-2\nu)+(1+\nu)(0.64/\phi)}\right)^2 - \phi\right] \Big/ (1-\phi) \quad (2)$$

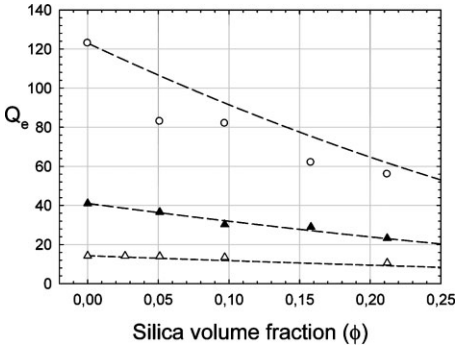

Figure 8.
Swelling equilibrium of hybrid hydrogels in $LiNO_3$ 0.5 mol/L versus the volume fraction of silica particles: SPx_PW0.14_R0 (○), SPx_PW0.14_R0.1 (▲) and SPX_PW0.14_R1 (△). Comparison with the theoretical model of Berriot[46] (dash line).

with ϕ the volume fraction of filler particles, Q_{ref} the swelling equilibrium of the organic matrix (SP0 hydrogels) and $\nu = 0.5$ the Poisson coefficient of hydrogels.

As shown in Figure 8, the resulting fits based on this model are rather good for the 3 series of hydrogels, in agreement with the adhesion behaviour of the PDMA matrix with the silica particles. The level of accuracy is less good for the R0 series as 1) the cross-linking reaction occurs only through uncontrolled transfer reactions and not by addition of a controlled amount of cross-linker and 2) the accuracy is rather weak for the swelling value of the unfilled hydrogel which swell a lot in aqueous media. This simple test of swelling confirms that the attractive interactions between PDMA and silica particles are effective within these hybrid hydrogels and we will investigate in the following part the consequences of this driving force on the mechanical properties

Mechanical Properties

The large strain behavior of hybrid hydrogels was investigated by uniaxial tensile tests for the 3 series of gels with x varying from 0 to 5 and z from 0 to 1 mol%. Typical stress-strain curves obtained at 0.06 s^{-1} are shown in Figure 9a in the case of SPx_PW0.14_R1.

Interestingly, we can notice that reversible interactions between PDMA chains and silica particles greatly enhance the mechanical properties of hydrogels, not only increasing the hydrogel stiffness, but also the nominal strain at failure. For instance, the initial modulus determined at low strain increases more than 5 times from SP0 to SP5, while the mean strain at failure is also improved by a factor 4. This general behavior of silica/PDMA hydrogels,[39] is a remarkable result in the field of nanocomposite materials and especially in NC gels as generally stiffness and deformability are antagonistic properties.[47–49] A simple estimation of the work of extension, given by the area under the tensile curve, yields $W \cong 1$ and 40 $kJ.m^{-3}$ for SP0 and SP5,

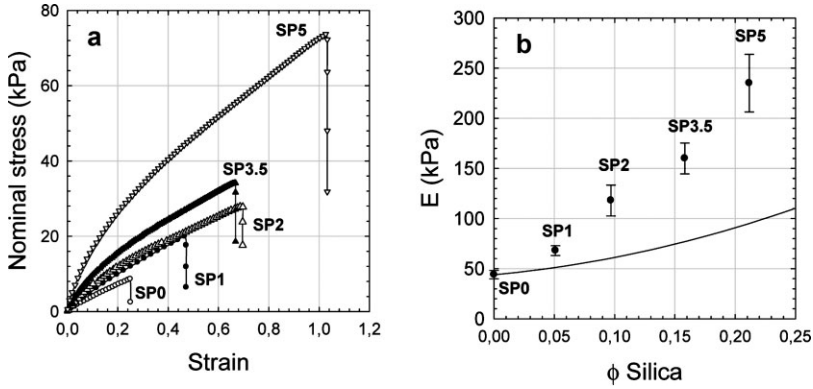

Figure 9.
Variation of the tensile mechanical behavior ($\dot{\varepsilon} = 0.06\,s^{-1}$) of "SPx_PW0.14_R1" hydrogels (a) and their initial modulus (b) as a function of silica particles. Guth and Gold predictions are represented as a continuous line with $E_0 = 44$ kPa obtained from the SP0 sample.

respectively, showing that physical interactions efficiently dissipate energy during the fracture process.

The role of physical interactions is emphasized in Figure 9b where the modulus of hydrogels, determined at low strain, is plotted versus the silica volume fraction and compared with the Guth and Gold model:

$$E = E_0\left(1 + 2.5\phi + 14.1\phi^2\right) \quad (3)$$

with E, the modulus of the reinforced material, E_0, the modulus of the unfilled matrix and ϕ, the volume fraction of filler.

As we can see, this hydrodynamic model which considers hard spherical particles embedded into an incompressible matrix without any interaction greatly underestimates the experimental results. The difference between experimental and calculated values is obviously related to the contribution of additional interactions between PDMA chains and silica particles and the Guth and Gold equation can be modified to take into account the modulus of the transient network (E_{Si}), proportional to the concentration of physical cross-links:

$$E = E_0\left(1 + 2.5\phi + 14.1\phi^2\right) + E_{Si} \quad (4)$$

Assuming the additivity of the contributions, this equation highlights the possibility to tune the hydrogel stiffness playing either with the physical interactions (SP ratio) or with the parameters of the covalent network like the degree of covalent crosslinking. This has been investigated with similar hybrid hydrogels prepared with smaller amount of crosslinker (R0.1 series) or without crosslinker (R0 series). As we can see in Figure 10, the self-crosslinked hybrid hydrogels (R0 series) are very soft and highly deformable as all the samples of this series can withstand high deformations (higher than 1000%) without breaking (Figure 10a). Nevertheless, it is noteworthy that while the unfilled sample SP0_PW0.14_R0 is too soft and sticky to be properly handled in tensile experiments (E was estimated at 1 kPa from rheometry), the hybrid gels of the same series really behave as viscoelastic materials with reinforced mechanical properties (Figure 10b).

On the other hand, the R0.1 series, prepared with a low but controlled level of MBA, display an intermediate behaviour with a modulus of 100 kPa for the SP5 sample and a quite large strain at break that reaches about 700%. We have to mention that strain at break determined from simple tensile tests have to be considered above all qualitatively as the crack initiation is very sensitive to the presence of defects in the sample. Nevertheless, fracture mechanics experiments performed on notched samples have not shown large discrepancies with

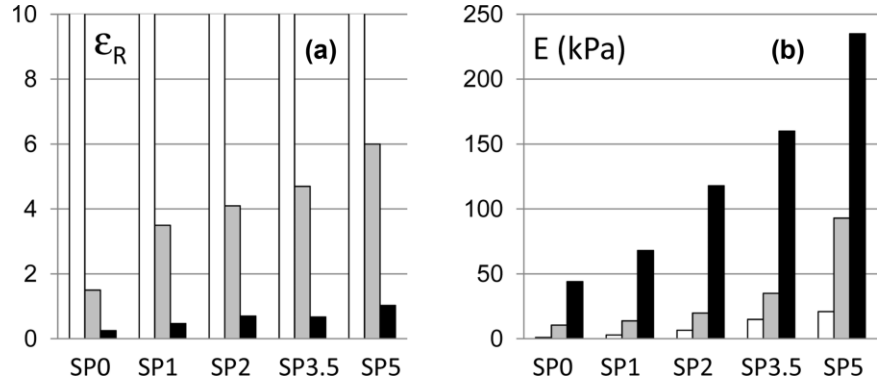

Figure 10.
Influence of silica particles on elongation at break (a) and Young modulus (b) for hybrid hydrogels prepared with different degree of cross-linking: R0 (□), R0.1 (■), and R1 (■).

standard tensile experiments. The general picture highlighted in Figure 10 is that both stiffness and strain at break are improved with increasing amount of silica particles, whatever is the degree of covalent cross-linking. This confirms the previous statement concerning the possibility to independently tune the covalent and the associating networks. By comparison with hybrid assemblies studied previously, the elastic reinforcement is much higher in the case of hybrid hydrogels, not only because the polymer concentration is higher but also because all the monomer segments of the polymer network are potential stickers towards the silica beads.

As physical interactions are reversible in nature, with characteristic time, the adsorption/desorption process of PDMA chains on silica surfaces can be studied by applying cycling tests at different velocities or stress relaxation experiments on longer timescales. Typical strain-controlled tensile loading/unloading cycles performed at intermediate velocity ($\dot{\varepsilon} = 0.06\,s^{-1}$) is shown in Figure 11.

These cycles performed in the low deformation range (from $\varepsilon_0 = 0$ to 0.1) clearly show the impact of particle/polymer associations with a strong increase of dissipated strain energy (area within the loop) with increasing amount of silica, as already reported on hybrid gels[37,39] or NC gels.[50,51] Without particles, the gel SP0 is only elastic; the dissipation of the matrix is negligible and the sample immediately recovers its initial dimension after unloading. Conversely, the hybrid SP5 shows a high hysteresis in these experimental conditions with some residual strain just after unloading (2%) but the material is able to recover its initial shape at rest within 10 seconds. Time is obviously a critical parameter in associating systems and this can be analyzed by changing the strain rate of loading/unloading cycles. In the case of the hydrogel SP5_PW0.14_R0.1 which has been recently studied in details,[39] a decrease of the dissipated energy from 5.4 to 0.2 $kJ \cdot m^{-3}$ was observed by changing the strain rate from very fast ($\dot{\varepsilon} = 0.6\ s^{-1}$) to

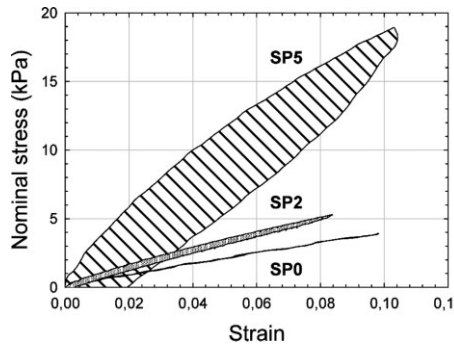

Figure 11.
Effect of silica content on the first loading-unloading cycle ($\varepsilon_o \cong 0.1$ at $\dot{\varepsilon} \sim 0.06\ s^{-1}$) for SPx_PW0.14_R1 hydrogels.

very slow ($\dot{\varepsilon} = 3.10^{-4}$ s^{-1}). Interestingly, it was shown in that case that the initial modulus was also a function of the strain rate ($E = 170$, 93 and 22 kPa at $\dot{\varepsilon} = 0.6$, 0.06 and 3.10^{-4} s^{-1}), the value obtained at very low strain rate being very close to the modulus calculated from the Guth and Gold model (equation {3}). This means that while the physical interactions, here reversible adsorption of PDMA on silica surfaces, efficiently reinforce the mechanical properties of the covalent network on short timescales, they mainly vanish on longer times.

By comparison with hybrid assemblies where we did not really observe relaxation phenomenon within the experimental conditions, the higher dynamics that seems to occur in hybrid hydrogels can be correlated to two main effects.

First of all we have to consider that hybrid hydrogels, which have been prepared with crude silica suspension around pH 9.5, are studied in these conditions while hybrid assemblies were formulated at pH 8 by mixing graft copolymer and ultra-filtered silica particles. As dissociation of silanol groups, initially involved in hydrogen bonding, increases with pH, OH^- can be regarded as a displacer towards polymer adsorption. For example, in the case of poly(ethylene oxide) [PEO] with silica particles, it was shown that the decrease of the adsorption energy above pH 8 was responsible for a decrease of 20% of the adsorbed amount of PEO between pH 8 and 9.2.[52] pH does not only modify the binding energy of polymer chains and adsorption properties at equilibrium but also the exchange dynamics.

The second point that must be considered is the local polymer concentration in the environment of silica particles. Even if most of the studies have been performed in excess of polymer chains, and especially in the case of hybrid hydrogels, it turns out that the dynamics of adsorption/desorption is greatly enhanced if more polymer chains are available in the immediate surroundings of the particles. Indeed, the adsorption/desorption process proceeds mainly through self exchange between adsorbed and free chains.[53] As the polymer concentration in hybrid assemblies is 5 to 50 times lower than in hybrid hydrogels, it is reasonable to expect a slower exchange dynamics for the former system.

Conclusion

Based on specific interactions taking place between PDMA and silica nanoparticles, we demonstrate that hybrid formulations with enhanced viscoelastic properties can be readily obtained following two main strategies. A comparison between the two hybrid systems is summarized in Figure 12 on the basis of simple mechanical analogues. The liquid viscoelastic behaviour of hybrid assemblies can be summarized by a Maxwell model involving a spring and a dashpot in series. These systems are liquid in nature, as there is no covalent cross-link between macromolecular chains, but the dynamics of the adsorption/desorption process of PDMA chains could be quite slow within the experimental conditions of pH and polymer concentration. Following this strategy, we show that a good knowledge of the binary complex "polymer side-chains/particles" is essential to anticipate the viscoelastic properties of the physical network. The key parameter is the "stoichiometry" of the complex PDMA/silica which corresponds to the plateau value of the adsorption isotherm. As a matter of fact, the maximum amount of

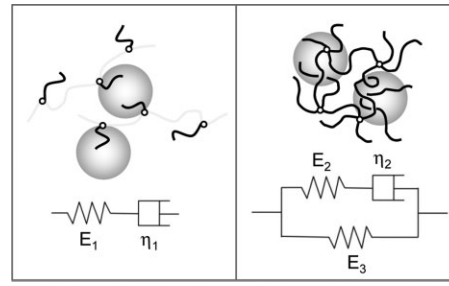

Figure 12.
Hybrids formulations together with their mechanical analogues.

adsorbed side-chains per surface unit is very useful to optimize the viscoelastic properties of hybrid formulations. Below and above the "stoichiometry", the concentration of elastically active chains progressively decreases and the rheological behaviour of hybrid mixtures turns from gel-like to liquid-like when large excess of organic or inorganic materials are added. Due to the strong interactions taking place between organic and inorganic materials, this efficient strategy remains limited at low polymer concentrations ($Cp < 20\,g{\cdot}L^{-1}$).

Conversely, hybrid hydrogels, prepared by polymerization of DMA in silica suspension, behave as viscoelastic solids since covalent cross-links are also introduced in the polymer matrix. Then, the mechanical behaviour can be schematically described on the basis of a Zener model coupling a spring and a Maxwell element in parallel. The spring holds for the elastic contribution of the organic cross-linked network, while the Maxwell element considers the time dependence of the physical contribution of PDMA/silica interactions to the Young modulus (E_{Si} in equation {4}). While the properties of the Maxwell element can be tuned with silica concentration or other parameters affecting the characteristics of the physical network (number of physical connections and/or their lifetime), the intrinsic elasticity of the covalent network can be controlled through structural parameters like polymer concentration and/or degree of cross-linking. The experiments reported in this paper clearly emphasize the possibility to design hybrid hydrogels with reinforced mechanical properties by playing with the balance between covalent and physical interactions. Contrary to former hybrid assemblies that cannot be easily prepared above $C_p = 20\,g{\cdot}L^{-1}$, the preparation of hybrid hydrogels requires a minimum polymer concentration of $50\,g{\cdot}L^{-1}$ in order to get homogeneous cross-linked networks.

[1] "*Water-soluble polymers, synthesis, solution properties and applications*"; In: S. W., Shalaby, C. L., McCormick, G. G. Butler, Eds., ACS Symposium Series 467 American Chemical Society, Washington DC **1991**.
[2] R. G. Larson, in: "*The Structure and Rheology of Complex Fluids*"; Oxford University Press, New York **1999**.
[3] D. A. Z. Wever, F. Picchioni, A. A. Broekhuis, *Progress in Polymer Science* **2011**, *36*, 1558–1628.
[4] I. Iliopoulos, T. K. Wang, R. Audebert, *Langmuir* **1991**, *7*, 617–619.
[5] A. Hill, F. Candau, J. Selb, *Prog. Colloid Polym. Sci.* **1991**, *84*, 61–65.
[6] T. Annable, R. Buscall, R. Ettelaie, D. J. Whittlestone, *J. Rheol.* **1993**, *37*, 695–726.
[7] A. Yekta, B. Xu, J. Duhamel, H. Adiwidjaja, M. A. Winnik, *Macromolecules* **1995**, *28*, 956–966.
[8] F. Petit, I. Iliopoulos, R. Audebert, S. Szonyi, *Langmuir* **1997**, *13*, 4229–4233.
[9] N. Cathebras, A. Collet, M. Viguier, J.-F. Berret, *Macromolecules* **1998**, *31*, 1305–1311.
[10] K. C. Tam, M. L. Farmer, R. D. Jenkins, D. R. Basset, *J. Polym. Sc. : Part B: Polym. Phys.* **1998**, *36*, 2275–2290.
[11] E. J. Regalado, J. Selb, F. Candau, *Macromolecules* **1999**, *32*, 8580–8588.
[12] K. Podhajecka, K. Prochazka, D. Hourdet, *Polymer* **2007**, *48*, 1586–1595.
[13] F. Tanaka, *Macromolecules* **1988**, *21*, 2189–2195; **1989**, *22*, 1988–1994; **1990**, *23*, 3784–3790.
[14] L. Leibler, M. Rubinstein, R. H. Colby, *Macromolecules* **1991**, *24*, 4701–4707.
[15] A. N. Semenov, J. F. Joanny, A. R. Khokhlov, *Macromolecules* **1995**, *28*, 1066–1075.
[16] A. N. Semenov, M. Rubinstein, *Macromolecules* **1998**, *31*, 1373–1385; 1386–1397.
[17] M. Rubinstein, A. N. Semenov, *Macromolecules* **2001**, *34*, 1058–1068.
[18] E. Siband, Y. Tran, D. Hourdet, *Macromolecules* **2011**, *44*, 8185–8194.
[19] A. Koike, N. Nemoto, T. Inoue, K. Osaki, *Macromolecules* **1995**, *28*, 2339–2344.
[20] B. T. Stokke, K. I. Draget, O. Smidsrød, Y. Yuguchi, H. Urakawa, K. Kajiwara, *Macromolecules* **2000**, *33*, 1853–1863.
[21] D. Portehault, L. Petit, N. Pantoustier, F. Lafuma, D. Hourdet, *Coll. Surf. A* **2006**, *78*, 26–32.
[22] L. Petit, L. Bouteiller, A. Brûlet, F. Lafuma, D. Hourdet, *Langmuir* **2007**, *33*, 147–158.
[23] L. Petit, C. Karakasyan, N. Pantoustier, D. Hourdet, *Polymer* **2007**, *48*, 7098–7112.
[24] D. Hourdet, L. Petit, *Macromol. Symp.* **2010**, *291–292*, 144–158.
[25] N. A. Peppas, *Hydrogels in Medicine and Pharmacy*. CRC Press, Boca Raton, FL **1986**.
[26] F. L. Buchholz, A. T. Graham, *Modern Superabsorbent Polymer Technology*. Wiley-VCH, **1997**.
[27] T. R. Hoare, D. S. Kohane, *Polymer* **2008**, *49*, 1993–2007.
[28] J. K. Oh, R. Drumright, D. J. Siegwart, K. Matyjaszewski, *Prog. Polym. Sci.* **2008**, *33*, 448–477.

[29] J. P. Gong, Y. Katsuyama, T. Kurokawa, Y. Osada, *Adv. Mater.* **2003**, *15*, 1155–1158.
[30] Y. Okumura, K. Ito, *Adv. Mater.* **2001**, *13*, 485–487.
[31] T. Matsunaga, T. Sakai, Y. Akagi, U. I. Chung, M. Shibayama, *Macromolecules* **2009**, *42*, 6245–6252.
[32] G. Miquelard-Garnier, C. Creton, D. Hourdet, *Soft Matter* **2008**, *4*, 1011–1023.
[33] S. Abdurrahmanoglu, V. Can, O. Okay, *Polymer* **2009**, *50*, 5449–5455.
[34] A. Haque, T. Kurokawa, G. Kamita, J. P. Gong, *Macromolecules* **2011**, *44*, 8916–8924.
[35] K. Haraguchi, T. Takehisa, S. Fan, *Macromolecules* **2002**, *35*, 10162–10171.
[36] K. Haraguchi, R. Farnworth, A. Ohbayashi, T. Takehisa, *Macromolecules* **2003**, *36*, 573265741.
[37] L. Carlsson, S. Rose, D. Hourdet, A. Marcellan, *Soft Matter* **2010**, *6*, 3619–3631.
[38] W. C. Lin, W. Fan, A. Marcellan, D. Hourdet, C. Creton, *Macromolecules* **2010**, *43*, 2554–2563.
[39] S. Rose, A. Dizeux, T. Narita, D. Hourdet, A. Marcellan, *Macromolecules* **2013**, doi: 10.1021/ma400447j.
[40] H. D. Bijsterbosch, M. A. Cohen Stuart, G. J. Fleer, *Macromolecules* **1998**, *31*, 8981–8987.
[41] E. A. S. Doherty, K. D. Berglund, B. A. Buchholz, I. V. Kourkine, T. M. Przybycien, R. D. Tilton, A. E. Barron, *Electrophoresis* **2002**, *23*, 2766–2776.
[42] P. Zhang, J. Ren, *Analytica Chimica Acta* **2004**, *507*, 179–184.
[43] H. H. Winters, M. Mours, *Advances in Polymer Science* **1997**, *134*, 165.
[44] R. Tanaka, J. Meadows, D. A. Williams, G. O. Phillips, *Macromolecules* **1992**, *25*, 1304–1310.
[45] T. Suzuki, H. Endo, N. Osaka, M. Shibayama, *Langmuir* **2009**, *25*, 8824–8832.
[46] J. Berriot, H. Montes, F. Lequeux, D. Long, P. Sotta, *Macromolecules* **2002**, *35*, 9756–9762.
[47] K. Haraguchi, H. J. Li, *Macromolecules* **2006**, *39*, 1898–1905.
[48] Y. Liu, M. F. Zhu, X. L. Liu, W. Zhang, B. Sun, Y. M. Chen, H. J. P. Adler, *Polymer* **2006**, *47*, 1–5.
[49] Y. T. Wu, M. G. Xia, Q. Q. Fan, Y. Zhang, H. Yu, M. F. Zhu, *J. Polym. Sci. Pt. B-Polym. Phys.* **2011**, *49*, 263–266.
[50] L. J. Xiong, X. B. Hu, X. X. Liu, Z. Tong, *Polymer* **2008**, *49*, 5064–5071.
[51] A. K. Gaharwar, S. A. Dammu, J. M. Canter, C. J. Wu, G. Schmidt, *Biomacromolecules* **2011**, *12*, 1641–1650.
[52] G. P. Van de Beek, M. A. Cohen-Stuart, *J. Phys. France* **1988**, *49*, 1449–1454.
[53] M. M. Santore, *Current Opinion in Colloid & Interface Science* **2005**, *10*, 176–183.

